P-ISSN 2586-9000
E-ISSN 2586-9027
Homepage : https://tci-thaijo.org/index.php/SciTechAsia
Science & Technology Asia
Vol.27 No.3 July - September 2022
Page: [121-131]
Original research article

Dolomite Characteristic from Natural Material and its Application as an Antibacterial

Lydia Rohmawati[1,*], Setya Permata Sholicha[1], Istiqomah[1], Woro Setyarsih[1], Munasir[1], Darminto[2]

[1]*Department of Physics, Faculty of Mathematics and Sciences, Universitas Negeri Surabaya, Surabaya 60231, Indonesia*
[2]*Department, of Physics, Faculty of Mathematics and Sciences, Institut Teknologi Sepuluh Nopember, Surabaya 60111, Indonesia*

Received 23 July 2020; Received in revised form 5 September 2021
Accepted 30 September 2021; Available online 29 September 2022

ABSTRACT

The remaining food left in the human oral cavity may cause bacteria to grow and develop more efficiently so that it will cause various oral diseases such as periodontitis, caries, and inflammation of the oral cavity. Bacteria that develop in the human oral cavity include *Staphylococcus aureus*, *Escherichia coli*, and *Streptococcus mutans*. Concerning the phenomenon, dolomite contains $CaCO_3$/MgO, of which the compound can be used as an antibacterial material because of its ability to inhibit bacterial activity. Dolomite preparation was carried out by heating at a temperature of 700°C for 1 hour. The calcined powder obtained was characterized by XRD, BET, FTIR, and TEM and used in antibacterial testing. Characterization results showed that dolomite consists of 47.1% $CaCO_3$ and 35.9% MgO, with a dolomite powder particle size of 49.49 nm. The surface area of dolomite powder was 174.154 m^2/g with a pore size of 84.94708 - 264.4389 nm, classified in the macropore category. Increase absorption at 500 cm^{-1} and 530 cm^{-1} corresponded to the MgO functional groups, and 1437 cm^{-1} corresponded to functional group of carbonate ions. Antibacterial activities of dolomite against *Staphylococcus aureus* and *Escherichia coli* bacteria were effective at a concentration of 40 g/liter. For the antibacterial activity against *Streptococcus mutans* bacteria, dolomite powder was effective at a concentration of 50 g/liter.

Keywords: Antibacterial activity; Characterization; Dolomite

***Corresponding author:** lydiarohmawati@unesa.ac.id

1. Introduction

In the human oral cavity, there are identified bacteria with about 700 microbial species [1, 2]. Microbial populations, including bacteria and fungi, can develop in the oral cavity [3]. Every human can hold 50-200 bacterial species [4], where these bacteria are found in saliva or biofilms on teeth or mucosa [5], on gingival epithelium or other inner surfaces in the oral cavity [6]. These pathogenic bacteria such as *Staphylococcus aureus*, *Escherichia coli*, and *Streptococcus mutans* quickly grow and develop in the human oral cavity because of some leftovers between the teeth [7]. These three bacteria can cause several oral cavity diseases including periodontitis, caries, and oral cavity inflammation. Bacterial growth can be inhibited by using the antibacterial substance derived from organic and inorganic compounds. Inorganic material has better stability than organic material; therefore, the study used inorganic materials such as dolomite [8]. Indonesia has abundant natural resources such as dolomite, located in the Bangkalan area of Madura Island. Dolomite compounds in Bangkalan area consist of 63.42% CaO, 26.39% MgO, 5.93% Na_2O, 1.20% SiO_2, 0.86% Al_2O_3 and 0.74% Fe_2O_3 [9]. MgO is an excellent antibacterial agent [10]. Heated dolomite is capable of producing CaO and MgO. Both compounds can be used as antibacterial agents because of the ability of $CaCO_3$/MgO to inhibit bacterial activity. Preparation of dolomite with heating at various temperatures of 600˚C, 700˚C and 800˚C for 1 hour, the results showed that the best $CaCO_3$/MgO composites were formed at 700˚C with an optimal phase percentage of MgO (periclase) and $CaCO_3$ (calcite) [11]. Dolomite preparations with variations in holding time up to 0.5 to 2.5 hours at 700˚C produced an optimal phase at 1 hour by producing 47.1% $CaCO_3$ and 35, 9 % MgO [12].

Based on the above reports, the purpose of this study was to investigate the characteristics of calcined dolomite, such as phase, particle and pore size distribution, peak absorption, and effectiveness of dolomite against bacteria. The results of this study are expected to prepare an antibacterial agent from dolomite.

2. Materials and Methods

2.1 Materials

The material used in this study was dolomite powder from Jaddih Bangkalan hill, Madura, East Java. Dolomite powder was mashed and sieved using a mortar pestle, and 200-mesh sieve. Calcination was carried out using a L5 / 11 / B170 furnace.

2.2 Dolomite calcination

Dolomite powder was crushed to an average particle size of about 7μm using mortar and pestle [11]. The dolomite powder was sieved and weighed then calcined at a temperature of 700°C for 1 hour. Subsequently, this powder was characterized by X-ray diffraction (XRD), Brunauer-Emmet-Teller (BET), Fourier Transform Infrared (FTIR), Transmission Electron Microscopy (TEM), and antibacterial activity.

2.3 Preparation antibacterial test

Antibacterial testing preparations included (1) dolomite powder resulting from calcination was dissolved with distilled water to form a suspension. After that, the powder solution was immersed in distilled water at 36°C, and pH was measured. (2) Each *Staphylococcus aureus*, *Escherichia coli*, and *Streptococcus mutans* were diluted with NaCl solution in a test tube, then homogenized using a vortex and standardized turbidity to a concentration of 0.5 Mc Farland. Each of these bacteria is applied to the media Mueller Hinton Agar (MHA). (3) A hole in the MHA media was made and the bacteria was inoculated. Subsequently, powder solution was added into each hole in the MHA media and incubated in an incubator at 37°C for 1 day,

2 days and 3 days. The diameter of the clear zone forming around the hole was measured using calipers. Dolomite mass variations used in this study were 5 g/liter, 10 g/liter, 15 g/liter, 20 g/liter, 25 g/liter, 30 g/liter, 35 g/liter, 40 g/liter, 45 g/liter and 50 g/liter with the tested bacteria including *Staphylococcus aureus* (Gram-positive bacteria), *Escherichia coli* (Gram-negative bacteria) and *Streptococcus mutans* (Gram-positive bacteria).

2.4 Instrumentation

The phase identification of dolomite samples was conducted with X-ray diffraction (XRD) using a PHILIPS-binary diffractometer equipped with CuKα radiation. The data were collected for scattering angles (2θ) ranging from 10 to 90° with a step size of 0.02°. Identification of the chemical bonding groups possessed by the test sample, which underwent heating in absorbing infrared light at a specific wavelength, was investigated from Fourier Transform Infrared (FTIR) results. The BET characterization tool used the Brunauer Emmet Teller (BET) Quantrachome TouchWin 1.2 engine. BET testing aims to determine the pore size and surface area of a sample. The tests were carried out with a heating temperature at 900˚C with nitrogen gas flowing into the sample to generate an adsorption curve. Transmission Electron Microscopy (TEM) tests were performed to determine the sample's morphology, diameter and particle size. The TEM tool used is JEM-1400.

3. Results and Discussion

3.1 Phase identification based on X-Ray Diffraction (XRD)

The results of XRD characterization were in the form of diffraction peak position data, the distance between fields (d) or commonly referred to as miller index and diffraction intensity (I). Analysis of XRD characterization was carried out using Match! Software, namely matching the ICSD database with MgO data (96-101-1118), $Ca(OH)_2$ (96-100-8782) and CaO (96-101-1096) with the XRD characterization data. The process of calcination on dolomite powder minimized the formation of impurities and could form new phases.

Fig. 1 showed the results of the XRD characterization on dolomite powder before and after calcination at 700˚C for 1 hour. The maximum intensity peak in dolomite samples after calcination was formed at an angle of 29.42 with the miller index (104), which was the calcite phase, while the MgO phase was found at the diffraction peak at an angle of 42.96 with the miller index (200). These results were similar to those previously reported in other studies [11]. The $CaCO_3$ phase was also formed at an angle of 36.00°, 47.53°, 48.50°, 57.43°, 60.96°, 64.69° with the miller index (110), (024), (122), (118), (012). Likewise, the MgO phase was formed at an angle of 62.32º, 74.66º, 78.66º with the miller index (021), (311), and (222). However, at 28º, 34º and 50º angles, the $Ca(OH)_2$ phase and an angle of 37º and 54º were the CaO phase. Both of these phases were impurities with low intensity. Dolomite powder before calcination showed some phase contents including 58.1% MgO, 23.1% $Ca(OH)_2$ and 10.8% CaO, while after calcination on dolomite powder, there were four phases formed, namely 47.1% $CaCO_3$, 35.9% MgO, 0.9% CaO and 16.6% $Ca(OH)_2$. The appearance of $Ca(OH)_2$ could be used as an anti-microbe and anti-fungal agent [13]. The CaO impurities could be used as antimicrobial substances because they contained the same superoxide, killing bacteria [14].

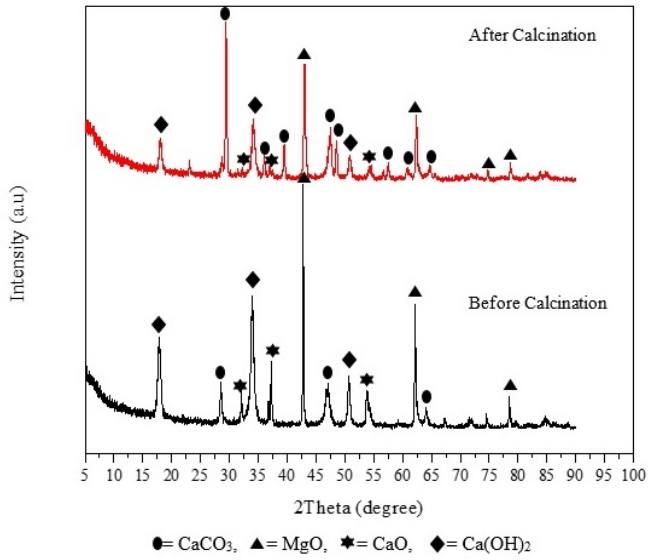

Fig. 1. XRD characterization of dolomite after calcination at 700˚C for 1 hour.

3.2 Pore size and pore surface area on dolomite based on Brunauer-Emmet-Teller (BET)

BET characterization was carried out to assign pore size and pore surface area on the dolomite as a result of calcination. The pore size was known from the adsorption curve through BJH (Barret Joyner Hallenda) data, as shown in Fig. 2. For antibacterial activities testing, the adsorption of bacteria by the material used in the oral cavity requires the proper pore size to inhibit bacteria's activity and not damage teeth. The ability to adsorb bacteria could be determined through the process of adsorption-desorption of nitrogen gas, wherein in this study, adsorption-desorption data were shown in an isotherm graph. Based on Fig. 3, the isotherm curve formed a hysteresis loop in the relative pressure range (0.95-0.99 P/Po). This isotherm curve belonged to the type II isotherm and belonged to the macropore category (d > 50 nm) [15]. The macropore size in this dolomite could facilitate the accessibility of bacteria in the adsorption surface [16].

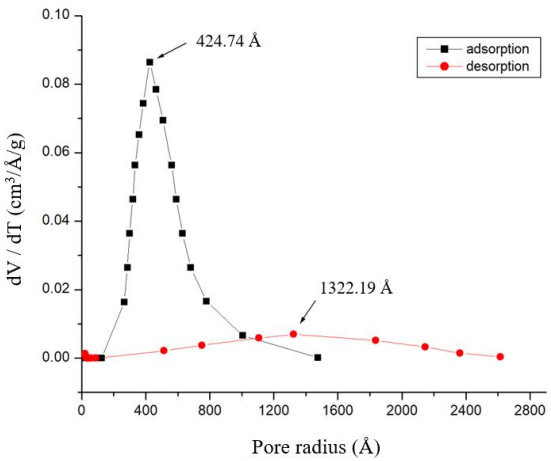

Fig. 2. Pore size distribution in dolomite powder based on the adsorption.

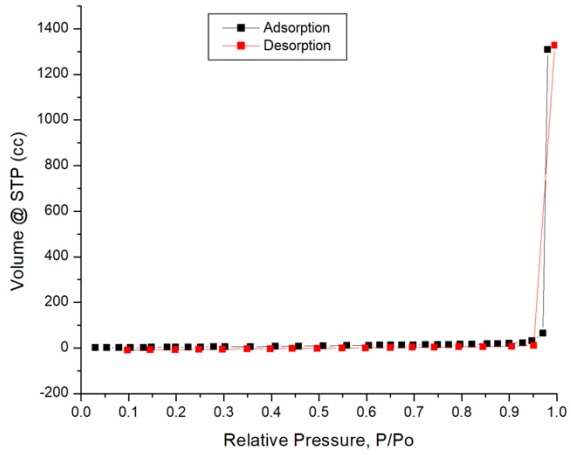

Fig. 3. Isotherm curve of sample dolomite powder.

3.3 Functional groups absorption based on FTIR

The results of FTIR characterization for dolomite before and after calcination had the same functional group absorption patterns with different intensities at wave numbers of 400 cm^{-1} to 4000 cm^{-1} (Fig. 4).

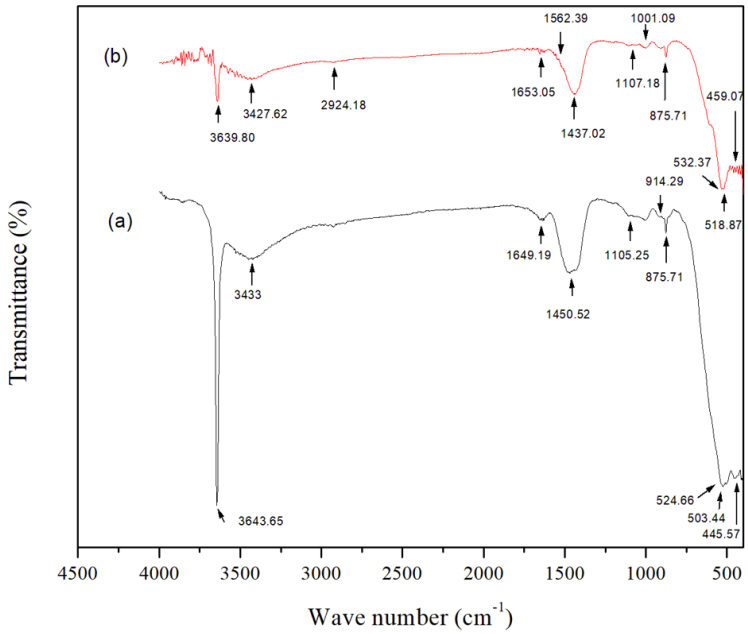

Fig. 4. FTIR characterization of dolomite powder before and after calcination.

Tables 1 and 2 show that wavenumbers 503 cm^{-1}, 530 cm^{-1} and 876 cm^{-1} indicate the presence of MgO stretching function groups. The absorption peaks at these wavelengths had similarities with the results of previous studies. It wavenumbers 511 cm^{-1} [17], 548 cm^{-1} [18] and 578 cm^{-1} [19], whereas between 500 cm^{-1} and 530 cm^{-1} in wavenumbers there was also an increase in absorption peaks in dolomite after calcination. The carbonate ion functional group could be found at wave number 1105

cm^{-1}. However, at 1001 cm^{-1} and 1437 cm^{-1}, an increase in absorption peaks indicated the presence of $CaCO_3$ functional groups in dolomite samples after calcination. The similarity of absorption peak in the wavenumber followed the results of several researchers, namely 1006 cm^{-1}, 1080 cm^{-1} [24] and 1404 cm^{-1} [18]. However, the wave number 1450 cm^{-1} was not found in dolomite samples after calcination, where the functional group indicated the presence of OH ions stretching and bending, which was characterized by the absorption of H_2O on metal surfaces [25]. Likewise, 1650 cm^{-1} and 3432 cm^{-1} experienced a significant decrease in absorption peaks for dolomite samples after calcination. At 1633 cm^{-1} and 3432 cm^{-1} are OH stretching and bending functional groups [26]. In addition, there was also a decrease in the absorption peak also at wave number 3640 cm^{-1} for dolomite samples after calcination, which was a functional group of $Ca(OH)_2$ in 3644 cm^{-1} [24]. Thus, dolomite after calcination based on the results of the FTIR test showed an increase in absorption for the functional groups of MgO and $CaCO_3$ and a decrease in the absorption peak of OH and $Ca(OH)_2$ ions.

Table 1. The results of FTIR dolomite powder characterization before calcination.

Atomic Bond	Wave Number (cm^{-1})	Reference Wave Numbers (cm^{-1})
MgO	445.57	443.63 [20]
MgO	503.44	548 [21]
		578 [19]
MgO	524.66	548 [21]
		578 [21]
MgO	875.71	882.18 [20]
$CaCO_3$	875.71	871.40 [18]
		875 [22]
MgO	914.29	882.18 [20]
$CaCO_3$	1105.25	1116 [23]
$CaCO_3$	1450.52	1388.46 [18]
$CaCO_3$	1649	1784.62 [18]
MgO	3433.41	3448.78 [20]
$CaCO_3$	3433.41	3430 [23]
$Mg(OH)_2$	3433.41	3440 [19]
MgO	3643.65	3887.54 [20]
$Mg(OH)_2$	3643.65	3700 [19]

Table 2. The results of FTIR dolomite powder characterization after calcined at 700 °C.

Atomic Bond	Wave Number (cm^{-1})	Reference Wave Numbers (cm^{-1})
MgO	459.07	443.63 [20]
MgO	518.87	548 [21]
		578 [19]
MgO	532.37	548 [21]
		578 [19]
MgO	875.71	882.18 [20]
$Mg(OH)_2$	875.71	825 [19]
$CaCO_3$	875.71	871.40 [18]
		875 [22]
$CaCO_3$	1001.09	1116 [23]
$CaCO_3$	1107.18	1116 [23]
$CaCO_3$	1437.02	1388.46 [18]
MgO	1437.02	1450 [25]
N-H Bending	1562.39	1543 [27]
$CaCO_3$	1653.05	1794.62 [18]
OH	1653.05	1633 [26]
CH Alifatik	2924.18	2920 [27]
MgO	3427.62	3448.78 [20]
$CaCO_3$	3427.62	3430 [23]
OH	3432	3432 [26]
$Mg(OH)_2$	3427.62	3440 [19]
MgO	3639.8	3887.54 [20]
$Mg(OH)_2$	3639.8	3700 [19]

3.4 Morphology and grain size of the nanometer dolomite powder

TEM characterization was performed on dolomite powder with the best percentage of $CaCO_3$ and MgO dominant phases at 1 hour holding time, where the TEM characterization on magnification 60.000 results showed the morphology and grain size of the nanometer dolomite powder. The two phases formed could be distinguished from their morphologies. The MgO phase was dark in color and circular shape, while the $CaCO_3$ phase was light-colored and box shape (Fig. 5). Using ImageJ software, the grain size in Fig. 5 for the $CaCO_3$ phase was in the range of 36 nm to 123 nm, while the grain size of the MgO phase ranged from 36 nm to 54 nm. The grain size of MgO proves that MgO was a nano-sized particle with a <100 nm, while $CaCO_3$ showed a size larger than MgO. According to Tang and Fang (2014), MgO nanoparticles could be formed by controlling the calcination temperature, which shows different grain sizes. Calcination temperature can affect the

morphology and size of MgO nanoparticles [10]. The grain size of these particles affects the antibacterial effectiveness, in which small particle size has a significant inhibition of bacterial.

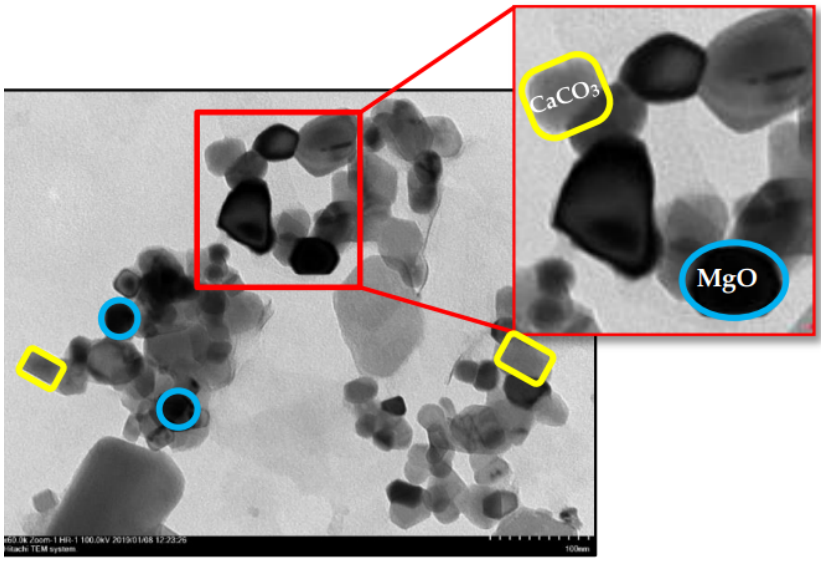

Fig. 5. Dolomite powder grain size at 1 hour holding time.

3.5 Antibacterial activity of dolomite

Antibacterial activity testing was carried out on dolomite powder to determine the inhibition zone of bacteria on the antibacterial material. Inhibitory zones formed around the wells indicated antibacterial effectiveness. The measurement of the inhibition zone diameter at 7.5 mm showed that the antibacterial activity against *Staphylococcus aureus* was most effective at two days with the dolomite concentration of 40 g/liter, while the antibacterial activity against *Escherichia coli* was most effective at one day and two days with the diameter of inhibitory zone of 5.5 mm at a concentration of 40 g/liter. Meanwhile, the diameter of the inhibition zone against *Streptococcus mutans* showed that the antibacterial activity was most effective at two days with a dolomite concentration of 50 g/liter at 6.75 mm (Table 3). Generally, the diameter of the inhibition zone tends to increase in proportion to the increase in the concentration of the antibacterial solution. However, Table 3 shows that the inhibition zone against *Staphylococcus aureus* bacteria decreased at the dolomite concentration from 45-50 g/liter on days 1 and 2. For *Escherichia coli* bacteria, the inhibition zone decreased at a concentration of 45-50 g/liter on day 1. In the inhibition zone, *Streptococcus mutans* bacteria also decreased for observation on day 1 at a concentration of 40-50 g/liter. The decrease in the inhibitory power of these bacteria was due to the lack of rate diffusion of antibacterial compounds (dolomite) into the agar medium [28]. The dilution factor influences the diffusion process. According to Valgas et al (2007), the deposition of antibacterial compounds causes a limited diffusion rate [29]. The higher the concentration of dolomite, the lower the solubility, so it can slow down the diffusion rate of dolomite into the media and consequently reduce the ability of dolomite with high concentrations to inhibit the

growth of bacteria such as *Escherichia coli*, *Staphylococcus aureus*, and *Streptococcus mutans*. Setha et al (2014) stated that when the concentration of antibacterial compounds is too high, the penetration of secondary metabolites into the bacterial cell wall can be disrupted, thereby reducing the effectiveness of antibacterial compounds in inhibiting bacteria [30]. The antibacterial effect can be time-dependent or concentration-dependent [31].

The decrease in the inhibition zone on day 3 for *Staphylococcus aureus* and *Escherichia coli* bacteria at a concentration of 40 g/liter, and *Streptococcus mutans* at a concentration of 50 g/liter, were because, on day three, the content of antibacterial compounds begins to decrease so that the ability to inhibit bacteria decreases. In addition, the antibacterial activity is only bacteriostatic. The bacteria began to adapt to the dolomite solution so that on the 3rd day, the solution did not affect bacteria. Bacteria began to be resistant to the dolomite solution so that bacterial growth occurred around the well. Thus, in this study, the optimum and efficient dolomite solution was used as a candidate for antibacterial material during the incubation period of 2 days. Following Yamamoto et al (2010) research, this result showed that the incubation of bacteria for two days decreased the number of bacterial colonies [32].

Table 3. Antibacterial activity of dolomite.

Concentration dolomite (g/liter)	Bacterial inhibitory zone diameter (mm)								
	S. aureus			*E. coli*			*S. mutans*		
	Day								
	1	2	3	1	2	3	1	2	3
5	0.00	0.00	0.00	0.00	0.00	0.00	0.00	0.00	0.00
10	1.00	1.25	2.25	1.50	1.75	1.25	1.50	1.25	1.25
15	2.00	0.75	1.50	2.50	1.50	1.00	1.50	1.25	1.25
20	1.50	0.00	0.00	2.25	2.00	2.25	3.00	0.00	0.00
25	3.50	3.50	3.25	2.02	2.50	2.50	3.50	1.75	1.75
30	3.52	3.50	2.25	3.52	5.00	3.00	3.00	3.00	2.25
35	3.50	4.25	2.75	3.75	2.50	1.75	4.50	4.75	3.25
40	6.75	7.50	3.75	5.50	5.50	2.25	4.25	5.00	3.00
45	3.75	3.25	3.00	4.00	4.00	0.75	3.75	4.25	3.00
50	4.50	5.50	4.50	4.50	5.50	4.25	2.50	6.75	5.25

Inhibition zones were formed on the media agar with each concentration of dolomite, indicating no bacterial growth in the area. The higher the concentration of a solution, the lower the growth of bacteria. The antibacterial material in this study belonged to the bacteriostatic group [33], where the antibacterial material inhibited the growth of bacteria but did not kill bacteria. Dolomite contain $CaCO_3$/MgO was an alkali metal oxide group, where the metal element can increase the pH of bacteria and superoxide (O_2^-) can exert pressure on the bacterial cell wall and bind to the cell membrane causing bacterial metabolism to be blocked [32], [34-35]. It can be seen that the antibacterial material from dolomite nanoparticles tends to be reactive to the types of Gram-positive and Gram-negative bacteria. The presence of CaO and $Ca(OH)_2$ in calcined dolomite contributes to antimicrobial activity. $Ca(OH)_2$ is an effective bactericide against pathogenic bacteria [36].

Similarly, CaO has antifungal and antibacterial activity against pathogenic bacteria [37]. Factors that may affect the inhibition of bacterial growth included the ability of adsorption by $CaCO_3$/MgO, where the adsorption was observed from the pore surface area and pore size of the material. The particle size possessed by antibacterial material was also a significant affecting the inhibition of bacteria. Antibacterial material is said to have good antibacterial activity if it has nanoparticles [9].

4. Conclusion

The phase formed by the heating of dolomite at a temperature of 700˚C holding time 1 hour was 47.1% $CaCO_3$ and 35.9% MgO. The particle size in dolomite powder was 49.49 nm with grain size for the $CaCO_3$ phase, ranging from 36 nm to 123 nm, whereas the grain size of the MgO phase ranged from 36 nm to 54 nm. Dolomite powder has a surface area of 174.154 m^2/g with a pore size of 84.94708 - 264.4389 nm, which was included in the macropore category. The antibacterial activity against *Staphylococcus aureus* is effective at two days after inoculation with the inhibition zone diameter of 7.5 mm at a concentration of 40 g/liter dolomite. The antibacterial activity against *Escherichia coli* was most effective in one day and two days after inoculation with the inhibition zone diameter of 5.5 mm at 40 g/liter concentration. The antibacterial activity against *Streptococcus mutans* bacteria was most effective at two days with a concentration of 50 g/liter at 6.75 mm.

Acknowledgements

The author conveys his gratefulness to the Ministry of Research and Higher Education of the Republic of Indonesia and the Department of Physics of Universitas Negeri Surabaya for allocating experimental facilities.

References

[1] Nada TH. Oral Microbiology in Periodontal Health and Disease; in Bhardwaj SB. Oral Microbiology in Periodontitis. IntechOpen Limited: London, United Kingdom; 2018. p.33-52.

[2] Palmer Jr RJ. Composition and development of oral bacterial communities. Periodontol 2000. 2014;64:20-39.

[3] Samaranayake LP, Matsubara VH. Normal Oral Flora and the Oral Ecosystem. Dent Clin North Am. 2017;61:199-215.

[4] Jacubovics NS, Burgess JG. Extracellular DNA in oral microbial biofilms. Microbes Infect. 2015;17:531-7.

[5] Staskova A, Nemcova R, Lauko S, Jenca A. Oral Microbiota from the Stomatology Perspective (Online First); in Dincer S, Ozdenefe MS, and Arkut A. Bacterial Biofilm (Working Title), IntechOpen Limited: London, United Kingdom; 2019. p. 1-22.

[6] Bui FQ, Almeida-da-Silva CLC, Huynh B, Trinh A, Liu J, Woodward J, Asadi H, Ojcius DM. Association between periodontal pathogens and systemic disease. Biomed J. 2019;42:27-35.

[7] Patil S, Rao RS, Amrutha N, Sanketh DS. Oral Microbial Flora in Health. World J Dent. 2013;4:262-6.

[8] Solihin S, Arini T, and Febriana E. Synthesis of Ultra Fine Grain Magnesium Carbonate Part 1. Calcination Behaviour of Indonesian Dolomite. Metalurgi. 2012;27:273-8.

[9] Sundrarajan M, Suresh J, Gandhi RR. Sol-Gel synthesis and characterization of magnesium peroxide nanoparticles Dig J Nanomater Biostructures. 2012;7:983-9.

[10] Sholicha SP, Sabrina GJ, Setyarsih W. Rohmawati L. Preparation of CaCO3/MgO from Bangkalan's dolomite for raw biomaterial. J Phys Conf Ser. 2019;1171:1-6.

[11] Rohmawati L, Sholicha SP, Holisa SPS. Setyarsih W. Identification of Phase CaCO3/MgO in Bangkalan Dolomite Sand as An Antibacterial Substance. J Phys Conf Ser. 2019;1417:1-5.

[12] Hapsari CA, Lutfi P, Ratu R, Novia R. J Polusi Tanah dan Air Tanah. 2012;1:1-9.

[13] Roy A, Gauri SS, Bhattacharya M, Bhattacharya J. Antimicrobial activity of

caO nanoparticles. J Biomed Nanotechnol. 2013;9:1570-8.

[14] Jannah Z, Mubarok H, Syamsiyah F, Putri AAH, Rohmawati L. Preparation of Calcium Carbonate (from Shellfish)/Magnesium Oxide Composites as an Antibacterial Agent. IOP Conf Ser-Mat Sci. 2018;367:1-6.

[15] Thommes M, Kaneko K, Neimark AV, Olivier JP, Reinoso FR, Rouquerol J, Sing KSW. Physisorption of gases, with special reference to the evaluation of surface area and pore size distribution (IUPAC Technical Report). Pure Appl Chem, 2015;87:1051-69.

[16] Ilomuanya MO, Nashiru B, Ifudu ND, Igwilo CI. Effect of pore size and morphology of activated charcoal prepared from midribs of Elaeis guineensis on adsorption of poisons using metronidazole and Escherichia coli O157:H7 as a case study. J Microsc Ultrastruct. 2017;5:32-8.

[17] Tamiselvi P, Yelilarasi A, Hema M, Anbarasan R. Effect of reduced graphene oxide (rGO) on structural, optical, and dielectric properties of Mg(OH) 2 /rGO nanocomposites. Nano Bulletin. 2013.

[18] Chen A, Luo Z, Akbulut M. Ionic liquid mediated auto-templating assembly of CaCO3-chitosan hybrid nanoboxes and nanoframes. Chem Commun (Camb). 2011;47:2312-4.

[19] Ansari A, Ali A, Asif M, Shamsuzzaman. Microwave-assisted MgO NP catalyzed one-pot multicomponent synthesis of polysubstituted steroidal pyridines. New J Chem. 2017;42:184-97.

[20] Sutapa IW, Wahab AW, Taba P, Nafie NL. Synthesis and Structural Profile Analysis of the MgO Nanoparticles Produced Through the Sol-Gel Method Followed by Annealing Process. Orient J Chem. 2018;34:1016-25.

[21] Kandiban M, Vigneshwaran P, Potheter IV. Proceeding of the National Conference on Advances in Crystal Growth and Nanotechnology (ACN 2015), C. M. S. College: Kottayam, Kerala; 15-16 January 2015.

[22] Reigh FB, Ad.elantado JVG, Moreno MCMM. FTIR quantitative analysis of calcium carbonate (calcite) and silica (quartz) mixtures using the constant ratio method. Application to geological samples. Talanta. 2002;58:811-21.

[23] Boke H, Akkurtb S, Ozdemir S, Gokturk EH, Saltik ENC. Quantification of CaCO3–CaSO3·0.5H2O–CaSO4·2H2O mixtures by FTIR analysis and its ANN model. Mater Lett. 2004;58:723-6.

[24] Shahraki BK, Mehrabi B, Dabiri R. Thermal behavior of Zefreh dolomite mine (Central Iran). J Min Metall. 2009;45B:35-44.

[25] Raghevandra M, Lalithamba HS, Shekarappa S, Hanumanaik R. Synthesis of Nα-protected formamides from amino acids using MgO nano catalyst: Study of molecular docking and antibacterial activity. Sci Iran Trans B. 2017;24:3002-13.

[26] Nurlaela A, Dewi SU, Dahlan K, Soejoko DS. Pemanfaatan Limbah Cangkang Telur Ayam dan Bebek sebagai Sumber Kalsium untuk Sintesis Mineral Tulang. J Pendidikan Fisika Indonesia. 2014;10:81-5.

[27] Tanasale MFJDP, Bandjar A, Sewit N. Isolasi Kitosan Dari Tudung Jamur Merang (Vollvariella Volvaceae) Dan Aplikasinya Sebagai Absorben Logam Timbal (Pb). Indo J Chem Res. 2018;6:556-62.

[28] Dawis WW, Stout TR. Disc Plate Method of Microbiological Antibiotic Assay. J Appl Microbiol. 1971;22:659-65.

[29] Valgas C, Machado de Souza S, Smânia EFA, Smânia Jr A. Screening methods to determine antibacterial activity of natural products. Braz J Microbiol. 2007;38:369-80.

[30] Setha B, Laga A, Mahendradatta M, Firdaus. 2014. Inhibition of Histamine Formation on the Frigate Tuna (Auxis Thazard Thazard, L) Using Leaf Extract of Jatropha curcas. Int J Sci Res. 2014;3:129-31.

[31] Pfaller MA, Sheehan DJ, Rex JH. Determination of Fungicidal Activities against Yeasts and Molds: Lessons Learned from Bactericidal Testing and the Need for Standardization. Clin Microbiol Rev. 2004;17:268-80.

[32] Yamamoto O, Ohira T, Alvarez K, Fukuda M. Antibacterial characteristics of CaCO3–MgO composites. Mater Sci Eng. 2010;173:208-12.

[33] Pankey GA, Sabath LD. Clinical relevance of bacteriostatic versus bactericidal mechanisms of action in the treatment of Gram-positive bacterial infections. Clin Infect Dis. 2004;38:864-70.

[34] Hewitt CJ, Bellara SR, Andreani A, Nebe-von-caron G, McFarlane CM. An evaluation of the anti-bacterial action of ceramic powder slurries using multi-parameter flow cytometry. Biotechnol Lett. 2001;23:667-75.

[35] Tag ZX, Lv BF. MgO nanoparticles as antibacteral agent: Preparation and activity. Braz J Chem Eng. 2014;31:591-601.

[36] Guerrero LC, Cervantes JG, Hernández DC, López RG, Guzmán SS, Cárdenas EC. Synthesis and Characterization of Calcium Hydroxide Obtained from Agave Bagasse and Investigation of Its Antibacterial Activity. Rev Int Contam Ambie. 2017;33:347-53.

[37] Roy A, Gauri SS, Bhattacharya M, Bhattacharya J. Antimicrobial activity of caO nanoparticles. J Biomed Nanotechnol. 2013;9:1570-8.